Theory and experiment on optical transverse intensity bistability in the transmission through a nonlinear thin (nematic liquid crystal) film

I. C. Khoo, P. Y. Yan,* T. H. Liu, S. Shepard, and J. Y. Hou†
Department of Physics and Astronomy, Wayne State University, Detroit, Michigan 48202
(Received 22 November 1983)

A theory is presented for the *transverse* intensity distribution bistability of a Gaussian optical beam after its passage through a nonlinear thin film. The equations governing the intensity distribution are cast in the form analogous to optical bistability in a longitudinal cavity (a Fabry-Perot interferometer), i.e., into two coupled transcendental equations from which multiple solutions are obtained. This formalism allows one to examine various physical approximations in obtaining the equations, and to improve on these approximations. It also lucidly illustrates the mechanisms of transverse intensity distribution bistability. The theoretical predictions are verified with quantitative experimental results on thin films of nematic liquid crystals.

Optical bistability has been a subject of intensive investigation recently.[1–5] Optical bistability in a system arises as a result of its nonlinear response to the input optical intensity, owing to some feedback from the output of the system. Intrinsic devices, where the feedback is purely optical, are usually based upon the Fabry-Perot cavities,[5,6] where the transmission is governed by the *longitudinal* intensity dependent phase shift. Depending on the relative magnitude of the optical input time, the material response time, and the cavity decay time, the behavior falls into a transient, quasisteady state and cw regimes.[7] Optical bistability has been shown to be an interesting phenomenon for the study of chaos,[4] and passage to chaos, and other fundamental as well as applied problems of optical switching and processing. A review of some of these processes has recently appeared.[3]

In this paper, we present the theory and experiment on a fundamentally different form of optical bistability, namely, bistability in the *transverse* intensity distribution of a laser beam after its passage through a nonlinear thin (nematic) film. Feedback is provided by a partially transmitting mirror at the output end. The theory developed here is generally applicable to other thin films. Theory for this type of so-called "external" self-focusing bistability[8] has been given before by Kaplan,[2] who essentially treated the film as a nonlinear thin lens with a focal length that is dependent on the optical intensity. In the theory to be described below, we make a further refinement by taking into account the total phase shift due to the thin film, and compare and contrast the results with expressions obtained under the lens approximation. More interestingly, the transverse intensity distribution is described by the solution to transcendental equations in a manner analogous to the case involving longitudinal phase shift. The occurrence of bistability switching (in the on-axis power, e.g.) can then be clearly represented as some switching back and forth between the on-axis intensity and the intensity at the wing of the Gaussian beam.

Theory and experiment on the so-called "strong self-focusing limit" bistability has been reported by Bjorkholm *et al.* In these studies, the nonlinear medium is rather thick so that the incident optical beam undergoes substantial wave-front reshaping within the nonlinear medium. For thin films, the nonlinearity gives rise simply to a phase factor in the otherwise undistorted wave front of the optical beam following its passage through the medium. Such a situation allows a more definitive imaging of the output (by the feedback mirror) back on the film using simple free space propagation description.

THEORY

Figure 1 depicts schematically the problem under study. A cw transversely Gaussian laser beam is incident with a radius of curvature R and beam waist ω on the nonlinear thin film. For a nematic film, the reorientation requires that the optical field be linearly polarized. The incident laser electric field is given by $\vec{E}_{op}(\vec{r},0)$. A lens L with a focal length f is situated a distance Z_0 from the thin film and a mirror with reflectivity R_m is placed a distance $Z_1/2$ from the lens. A pinhole of radius a and an identical lens of focal length f are placed a distance $(Z_0+Z_1/2)$ and $Z_1/2$, respectively (for convenience in calculation) behind the mirror. The output power (or intensity) through the pinhole is studied as a function of the total input power P_{in}.

The nonlinearity induced in the nematic film has been calculated before. In the case of a homeotropically aligned film of thickness d, with the incident optical wave vector making an angle ϕ with the nematic director, the induced refractive index change associated with the optically induced reorientation can be expressed in the form[9]

$$\Delta n(z)=\frac{\epsilon^{1/2}(\Delta\epsilon)^2\sin^2(2\phi)(dz-z^2)E_{op}^2}{16\pi K}$$
$$=\frac{\pi^2\epsilon^{1/2}\Delta\epsilon\sin^2(2\phi)}{4}\frac{E_{op}^2}{E_{th}^2}\frac{(dz-z^2)}{d^2}$$
$$=\frac{\pi^2\epsilon^{1/2}\Delta\epsilon\sin^2(2\phi)}{4}\left[\frac{dz-z^2}{d^2}\right]\frac{I_{op}}{I_{th}}, \quad (1)$$

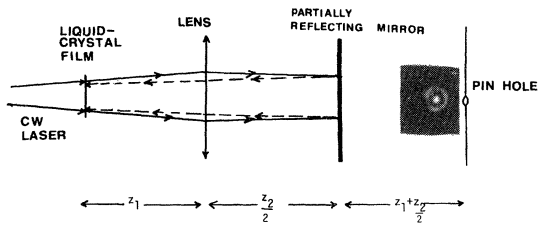

FIG. 1. Schematic of the transverse optical intensity distribution bistability experiment setup. Inset is an actual photo taken of the intensity distribution just after switching-up. Before switching, the intensity distribution is Gaussian.

where E_{op}^2 is the square modulus of the optical electric field in the nematic film and E_{th} is the so-called optical Fréedericksz transition threshold field:[9]

$$E_{th}=4\pi^3 K(\Delta\epsilon)^{-1}d^{-2} .$$

Notice that $\Delta n(z)$ is dependent on the distance (z) into the nematic film, a nonlocal optical nonlinearity.

It is interesting to note here that, peculiar to liquid crystals, the response (i.e., the reorientation) of the nematic director axis is also nonlocal in the transverse direction of the beam. Since the laser beam has a beam waist of about ω_0, the problem should be solved for this transverse direction subject to (approximately) the boundary condition that the reorientation is vanishing outside a region of transverse dimension ω_0. With respect to molecules outside this region, the molecules undergo basically a splay distortion. It suffices to note from (1), that the reorientation of the director axis is inversely proportional to the square of thickness of the sample (for the longitudinal boundary problem) and to ω_0 for the transverse direction. In the experiment, $\omega_0\approx 0.3$ mm (300 μm) while $d\approx 50$ μm, so that the reorientation of the director axis is more severely [by at least $(300^2/50)=36$ times] limited by the thickness of the sample, i.e., the transverse boundary effect is negligible, and thus a detailed calculation (which would be extremely complicated if the transverse Gaussian profile of the beam is explicitly accounted for) is not necessary for the present treatment. (Nevertheless, we have explicitly calculated this transverse nonlocal effect, and the lengthy calculation, which will be published in a later paper, confirms the above observation.) From Eq. (1) the induced refractive index change is of the familiar form

$$\Delta n=n_2(z)I_{op}(r) , \tag{2}$$

where n_2 can be deduced from (1).

This refractive index change produces a transversely dependent phase shift on the optical beam by an amount

$$\delta\phi(r)=\frac{2\pi}{\lambda}\int_0^d n_2(z)I(r)dz=\frac{2\pi}{\lambda}\bar{n}_2 dI(r) , \tag{3}$$

where $\bar{n}_2$ denotes the average over the thickness of the film. The total intensity in the sample is given by

$$I=\frac{C}{4\pi}(E_0+E_R)^2\rightarrow I_0+I_R , \tag{4}$$

where the interference term due to E_0 and E_R (the reflected optical electric field) is neglected because the liquid crystal undergoes vanishingly small reorientation for interference on the order of optical wavelength. This is slightly different from the usual third-order nonlinearity $\chi^{(3)}$ EEE which results in a factor of 2 for I_R.

For the sake of simplicity, we shall first neglect the presence of the lens in the following analysis. The effect of the lens is included in the next section. Using Huygen's principle, the exit beam electric field at a distance z from the nematic film is given by

$$E(r_0,z)=\frac{2\pi}{i\lambda z}\exp(ikz)\exp\frac{-ikr_0^2}{2z}\times\int_0^\infty E_0(r,0)\exp\frac{-ikr^2}{2z}J_0\left[\frac{2\pi r r_0}{\lambda z}\right]\times\exp[-i\delta\phi(r)]r\,dr , \tag{5}$$

where $r_0=(x_0^2+y_0^2)^{1/2}$ and $r=(x^2+y^2)^{1/2}$ and J_0 is the zeroth-order Bessel function. The incident electric field $E_0(r,0)$ is given by

$$E_0(r,0)=\sqrt{I_0}\exp\left[-\frac{r^2}{\omega^2}-\frac{ikr^2}{2R}\right] . \tag{6}$$

Squaring both sides of (5) with (6) substituted from $E(r,0)$ yield the output intensity distribution at the plane

$$I(r_0,z)=\left[\frac{2\pi}{\lambda z}\right]^2 I_0\left|\int_0^\infty dr\, rJ_0(2\pi r r_0/\lambda z)\exp(-r^2/\omega_0^2)\times\exp\left\{-ik\left[\frac{r^2}{2z}+\frac{r^2}{2R}+\bar{n}_2 I_0 d\exp\left[-\frac{2r^2}{\omega^2}\right]+\bar{n}_2 R_m dI(r,z)\right]\right\}\right|^2 . \tag{7}$$

Equation (7) is an integral equation for the intensity distribution $I(r,z)$ via the intensity-dependent phase shift factor in the integrand. This implies the possibility of multiple solutions for $I(r_0,z)$. We remark here that in the case of zero feedback ($R_m=0$) this expression allows one to calculate exactly the transmitted intensity distribution beam waist, effective focal distance, interference ring structure, etc. The calculation was performed for a nematic film and good quantitative agreements are obtained between the theoretical and experimental results.[10,11]

In the case of finite R_m, there is no closed form analytic solution for $I(r_0,z)$. However, by expanding the Bessel function in the integrand into an infinite series, some new insights can be gained and numerical solutions are possible. One can also examine various approximations and refinements to these approximations and how they may be reflected in the predicted bistability behaviors.

Writing

$$J_0(2\pi r r_0/\lambda z)=\sum_{s=0}^{\infty}\frac{(-1)^s}{s!}(\pi r r_0/\lambda z)^{2s} \tag{8}$$

and inserting it into (7), one gets

$$\begin{aligned}I(r_0,z)&=(k/z)^2 I_0\left|\int_0^{\infty} dr\, rJ_0(krr_0/z)\exp\{-r^2/\omega^2-k[r^2/2z+r^2/2R+dI_0\exp(-2r^2/\omega^2)+n_2 dR_m I]\}\right|^2\\&=(k/z)^2 I_0\left|\sum_{s=0}^{\infty}\frac{(-1)^s}{s!^2}(kr_0/2z)^{2s}\int_0^{\infty} dr\, r^{2s+1}\exp\{(-r^2/\omega^2)-ik[r^2/2z+r^2/2R+n_2 dI_0\exp(-2r^2/\omega^2)\right.\\&\qquad\left.+n_2 dR_m I]\}\right|^2 .\end{aligned} \tag{9}$$

By inspection, $I(r_0,z)$ is of the form

$$I(r_0,z)=\sum_{n=0}^{\infty}(-1)^n A_{2n} r_0^{2n} , \tag{10}$$

where we have

$$A_0=(k/z)^2 I_0\left|\int_0^{\infty} dr\, rf(r,z)\right|^2 \tag{11}$$

and

$$\begin{aligned}A_2=(k/z)^4\frac{I_0}{4}&\left[\int_0^{\infty} dr\, r^3 f(r,z)\int_0^{\infty} dr\, rf^*(r,z)\right.\\&\left.+\int_0^{\infty} dr\, r^3 f^*(r,z)\int_0^{\infty} dr\, rf(r,z)\right] ,\end{aligned} \tag{12}$$

where

$$\begin{aligned}f(r,z)=\exp\Bigg[&-r^2/\omega^2\\&-ik\Bigg[r^2/2z+r^2/2R-2n_2 I_0 d/\omega^2\\&\quad+n_2 dI_0\exp(-2r^2/\omega^2)\\&\quad+n_2 dR_m\sum_{n=0}^{\infty}A_{2n}r^{2n}\Bigg]\Bigg] .\end{aligned} \tag{13}$$

The infinite coupled [via the integral over $f(r,z)$ on the right-hand side (rhs)] transcendental equations for A_{2n} in general imply multiple solutions for the A_{2n} and therefore for the output intensity distribution.

(i) "Near axis" approximation

We now make a simplifying approximation (which will be partially removed in the Appendix) by including only the first two terms ($\propto A_0$ and A_2) in the feedback $I(r_0,z)$ and the incident intensity ($I_0\exp -2r^2/\omega^2$), i.e., the phase shift due to the total intensity

$$\delta\phi=\bar{n}_2 dI_0\exp\left[-r^2/\omega^2+\bar{n}_2 dR_m\sum_{n=0}^{\infty}A_{2n}r^{2n}\right]$$

is rewritten as

$$\delta\phi=\bar{n}_2 dI_0\left[1-\frac{r^2}{\omega_0^2}\right]+\bar{n}_2 dR_m(A_0+A_2 r^2) . \tag{14}$$

This assumption is equivalent to the usual lens approximation, where the total phase shift is represented by the quadratic (in r) phase shift associated with a spherical lens. In this approximation, we have

$$\begin{aligned}f(r,z)=\exp[&-r^2/\omega^2\\&-ik(r^2/2z+r^2/2R-2\bar{n}_2 I_0 r^2/\omega^2+\bar{n}_2 dI_0\\&\quad-\bar{n}_2 dR_m A_2 r^2+\bar{n}_2 dR_m A_0)]\\=\exp(&-Br^2)\exp[ik(\bar{n}_2 dR_m A_0-\bar{n}_2 dI_0)] ,\end{aligned} \tag{15}$$

where

$$B=\frac{1}{\omega^2}+ik\left[\frac{1}{2z}+\frac{1}{2R}-\bar{n}_2 dI_0\frac{2}{\omega^2}-\bar{n}_2 dR_m A_2\right] . \tag{16}$$

The integrals in (11) and (12) yield

$$\begin{aligned}A_0&=\left[\frac{k}{z}\right]^2 I_0\left|\frac{1}{2B}\right|^2\\&=\frac{I_0}{4z^2\left[\left[\frac{1}{\omega^2 k}\right]^2+\left[\frac{1}{2z}+\frac{1}{2R}-\frac{2\bar{n}_2 I_{0d}}{\omega^2}-n_2 dR_m A_2\right]^2\right]}\end{aligned} \tag{17}$$

and

$$\begin{aligned}A_2&=\left[\frac{k}{z}\right]^2\frac{I_0}{4}\left[\frac{1}{2B^2}\frac{1}{2B^*}+\frac{1}{2B^{*2}}\frac{1}{2B}\right]\\&=\left[\frac{k}{z}\right]^4\frac{I_0}{4}\frac{1}{4|B|^2}\left[\frac{1}{B}+\frac{1}{B^*}\right]\\&\quad+\left[\frac{k}{z}\right]^2\frac{I_0}{8}\frac{1}{|B|^2}\left[\frac{1/\omega^2}{|B|^2}\right] .\end{aligned} \tag{18}$$

Equation (17) for A_0 shows that it is dependent via the reflectivity R on A_2, i.e., the on-axis optical intensity is influenced by the intensity away from the axis, as a result of the feedback. This indicates the possibility of energy redistributions among the various radial positions. On the other hand, Eq. (18) for A_2 is a transcendental equation in A_2, clearly demonstrating the possibility of a multiple-

valued solution for A_2 (and therefore for A_0 via its dependence on A_2). More interestingly, if we introduce the variable

$$u=\omega^2 k(1/2z+1/2R-2n_2 I_0 d/\omega^2-n_2 d R_m A_2) \quad (19)$$

we can rewrite Eqs. (17) and (18) as

$$B_1-B_2 u=\frac{1}{(1+u^2)^2} \quad (20)$$

with

$$B_1=\frac{8z^4(1/2z+1/2R-2\bar{n}_2 I_0 d/\omega^2)}{R_m \bar{n}_2 I_0 d\omega^6 k^4} \quad (21)$$

and

$$B_2=\frac{8z^4}{R_m \bar{n}_2 I_0 d\omega^8 k^5} . \quad (22)$$

Equation (20) is a transcendental equation for u in a form analogous to the Fabry-Perot bistability problem, i.e., the solution(s) is (are) given by the intersection of a straight line $y=(B_1-B_2u)$ and a bell-shaped function $y=(1+u^2)^{-2}$. The slope of the straight line (B_2) is *inversely proportional* to the magnitude of the incident intensity, similar to that in the usual Fabry-Perot theory. The difference is that in this case the intercept B_1 also varies with I_0.

Figure 2 is a typical plot of Eq. (20) for values of y corresponding to experimental parameters close to those used in the experiment ($\omega=0.03$ cm, $R=1650$ cm, $R_m=0.99$, $\lambda=5145$ Å and $z=30$ cm, $d=50$ μm, $\phi=22.5°$). The straight lines 1, 2, and 3 correspond to $\Delta n=6\times10^{-4}$, 1.2×10^{-3} and 1.8×10^{-3}, respectively. $\bar{n}_2$ can be estimated from (1)–(3) to be roughly given by $\bar{n}_2=3\times10^{-5}$ cm^2 W^{-1} for $\Delta\epsilon=0.8$ and $K=10^{-7}$ cgs unit. So these three values of Δn correspond to $I_0=20$, 30, and 60 W/cm^2. The intersections of the two functions in Fig. 2 give the solutions for u (and therefore for A_0 and A_2). For the range of values of I_0 such that $n_d \le \Delta n \le n_a$, there are triple-valued solutions for u, where n_d and n_a denote the value of Δn (and therefore I_0) for switch-down and switch-up operation. The expressions for n_d and n_u can be obtained from Eq. (20). More interestingly, Fig. 3 gives the output power (integrated over the pinhole with $a=0.005$ cm) versus the input power for $z=30$, 35, and

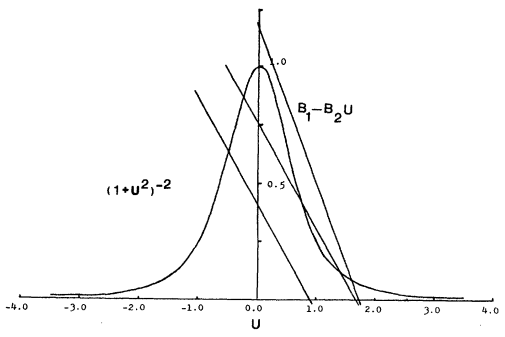

FIG. 2. Theoretical plot of the functions $y=B_1-B_2u$ and $y=(1+u^2)^{-2}$. Intersection(s) give the solution(s) for u.

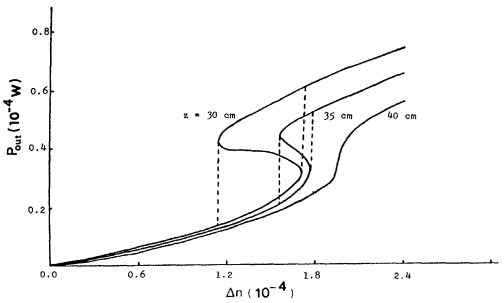

FIG. 3. Plot of the detected output power at the pinhole vs the change in refractive index $\Delta n=\bar{n}_2 I_0$.

40 cm. It clearly demonstrates the expected bistability switching for some value of z.

Figure 4 depicts the results for various values of the feedback mirror reflectivity R_m at $z=30$ cm. As expected, when R_m decreases, the switching powers increase.

As a refinement to the preceding analysis, we have taken into account the total phase shift due to the input beam, but still keep only the two leading terms in the contribution from the feedback beam. As shown in the Appendix, one can again express the resulting equations in transcendental equations. The multiple solutions (and bistability) for the intensity distribution obtained by including the total Gaussian phase shift is almost identical to the one obtained before. This demonstrates that for the first switching hysteresis loops, at least, the near axis approximation is quite good.

(ii) Bistability in the presence of a lens between the thin film and the feeback mirror

We now consider the effect of the lens between the liquid-crystal film and reflecting mirror M (cf. Fig. 1). This corresponds to the *actual* experimental setup. We label the distance between the liquid-crystal film and lens L_2 as z and distance between L_2 and reflecting mirror M as $z_1/2$ as shown in Fig. 5. Further, we let the output beam field at L_2 be E_1, the feedback beam field at L_2 be E_2, and the feedback beam field at liquid crystal be E_3. The Fresnel integral for the optical electric fields then gives

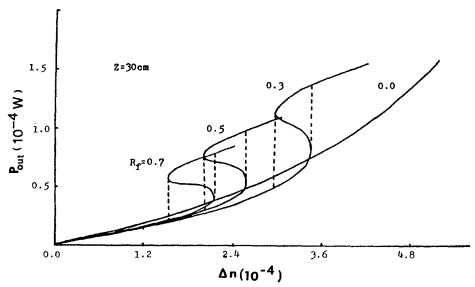

FIG. 4. Similar plot for various values of Rm, the mirror reflectivity.

$$E_1(r_0,z)=\left[\frac{k}{2}\right]\sqrt{I_0}\exp[i\phi(z)]\int_0^\infty dr\, rJ_0(krr_0/z)\exp\left[-r^2/\omega^2-ik\left[\frac{1}{2z}+\frac{1}{2R}-\frac{2\bar{n}_2I_0d}{\omega^2}-n_2dR_mA_2\right]r^2\right]$$
$$=\left[\frac{k}{z}\right]\sqrt{I_0}\exp[i\phi(z)]\frac{\exp(-k^2r_0^2/4z^2B)}{2B}, \tag{23}$$

where

$$B=1/\omega^2+ik(1/2z+1/2R-2\bar{n}_2dI_0/\omega^2-\bar{n}_2I_0R_mA_2) \tag{24}$$

and $\phi(z)$ is a phase factor which is only a function of z.

From Fourier optics,[10] we know that the effect of a lens is to change the optical field by a phase factor $\exp(ikr^2/2f)$ with f being the focal length, so the field right after L_2 is $E_1\exp(ikr^2/2f)$. An integral similar in form to (23) is obtained for E_2 which is given by

$$E_2(r_0,z,z_1)=\left[\frac{k}{z}\right]\left[\frac{k}{z_1}\right]\sqrt{I_0}\exp(i\phi_1)\times\frac{\exp(-k^2r_0^2/4z_1^2B_1)}{2B2B_1}, \tag{25}$$

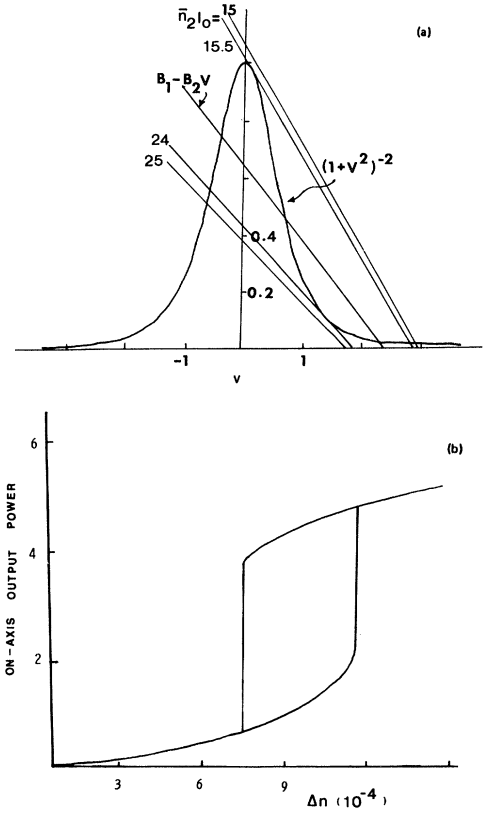

FIG. 5. (a) Theoretical plot of the function $y=B_1-B_2V$ and $y=(1+V^2)^{-2}$ for the case where the lens between the sample and the mirror is included in the calculation. Intersection(s) give value(s) for V. Parameters used are identical to the experimental setup. (b) Theoretical plot of the output vs input power for the parameters used in the experiment. Pinhole at the on-axis location. Note: $\bar{n}_2$ is estimated to be 3×10^{-5} in the text.

where

$$B_1=k^2/4z^2B-ik/2f+ik/2z_1 . \tag{26}$$

Similarly, the field E_2 acquires a phase factor $\exp(ikr^2/2f)$ after E_2 just passed through L_2 and we find that the field E_3 is given by, finally,

$$E_3(r_0,z,z_1)=\left[\frac{k}{z}\right]^2\left[\frac{k}{z_1}\right]\sqrt{I_0}\times\exp(i\phi_2)\frac{\exp(-k^2r_0^2/4z^2B_2)}{2B2B_12B_2}, \tag{27}$$

where

$$B_2=k^2/4z_1^2B_1-ik/2f+ik/2z . \tag{28}$$

The feedback intensity, therefore, is given by

$$I(r_0,z,z_1)=|E_3(r_0,z,z_1)|^2=\frac{k^6I_0}{z^4z_1^2}\left[\frac{\exp(-k^2r_0^2/4_z^2B_2)}{2^6BB_1B_2}\right]^2 . \tag{29}$$

After a few mathematical steps we find

$$|\exp(k^2r_0^2/4z^2B_2)|^2=\exp\left[\frac{-2b^2b_1\omega^2r_0^2}{(b_1-a_1a)^2+[(b-a_1a)u+ab\omega^2]^2}\right]$$
$$=1-\frac{2b^2b_1\omega^2r_0^2}{(b_1-a_1a)^2+[(b_1-a_1a)u+\omega^2ab]^2}+O(r^2) \tag{30}$$

and

$$\frac{1}{|BB_1B_2|^2}=\frac{\omega^4}{(b_1-a_1a)^2+[(b-a_1a)u+ab\omega^2]^2} \tag{31}$$

with

$$b=(k/2z)^2,\quad b_1=(k/2z_1)^2,$$
$$a=k/2z-k/2R,\quad a_1=k/2z_1-k/2f, \tag{32}$$
$$u=\omega^2k(1/2z+1/2R-2n_2I_0d/\omega^2-n_2dR_mA_2) .$$

Substituting (30) into (29), we obtain the output on-axis intensity distribution. (To simplify matters, we have assumed that there is another lens with focal length f, identical to L_2, that is placed at a distance $z_{1/2}$ measured from the other side of M and the output intensity is measured right after that lens with a pinhole placed at a distance z from the lens.) The output near axis intensity distribution is therefore given by

$$I(r,z,z_1)=A_0-A_2r^2 \tag{33}$$

with

$$A_0=(k^6/z^4z_1^2)\frac{I_0\omega^4}{2^6\{(b_1-a_1a)^2+[(b_1-a_1a)u+ba\omega^2]^2\}}, \tag{34}$$

$$A_2=(k^6/z^4z_1^2)\frac{2b_1b^2\omega^6}{2^6\{(b_1-a_1a)^2+[(b_1-a_1a)u+ba\omega^2]^2\}^2}. \tag{35}$$

Further, by letting $D_1=b_1-a_1a$ and introducing a new variable v defined by

$$v=\frac{D_1u+ab\omega^2}{D_1}, \tag{36}$$

(34) and (35) can further be reduced to

$$A_0=\frac{b_1b^2I_0\omega^4}{D_1^2(1+V^2)}, \tag{37}$$

$$A_2=\frac{zb^4b_1^2I_0\omega^6}{D_1^4(1+V^2)^2} \tag{38}$$

(note: $k^6/z^4z_1^2=2^6\pi^6/\lambda^6z^4z^2=2^6b^2b_1$). From definition of v we have

$$u=\frac{d_1V-ab\omega^2}{D_1}.$$

Further by the definition of u, we have

$$\frac{1}{2z}+\frac{1}{2k}-\frac{2\bar{n}_2I_0d}{\omega^2}-n_2dR_mA_2=\frac{D_1v-ab\omega^2}{D_1k\omega^2}, \tag{39}$$

$$n_2dR_mA_2=\frac{1}{2z}+\frac{1}{2R}-\frac{2\bar{n}_2I_0d}{\omega^2}+\frac{ab}{kD_1}-\frac{v}{k\omega^2}.$$

Substituting (7) into (6) yields

$$\begin{aligned}\frac{1}{(1+v^2)^2}&=\frac{D_1^4}{2b^4b_1^2I_0\omega^6n_2dR_m}\left[\frac{1}{2z}+\frac{1}{2R}-\frac{2n_2I_0d}{\omega^2}+\frac{ab}{kD_1}-\frac{v}{\omega^2}\right]\\&=\frac{D_1^4}{zb^4b_1^2I_0\omega^6n_2dR_m}\left[\frac{1}{2z}+\frac{1}{2R}-\frac{2n_2I_0d}{\omega^2}+\frac{ab}{kD_1}\right]\\&\quad-\frac{D_1^4}{2b^4b_1^21_0\omega^6n_2dk\,\omega^2R_m}v,\end{aligned} \tag{40}$$

i.e., we have

$$\frac{1}{(1+v^2)^2}=B_1-B_2v \tag{41}$$

with

$$B_1=\frac{D_1^4}{2b_1^2b^4I_0\omega^6n_2dR_m}\left[\frac{1}{2z}+\frac{1}{2R}-\frac{2\bar{n}_2I_0d}{\omega^2}+\frac{ab}{kD_1}\right], \tag{42}$$

$$B_2=\frac{D_1^4}{2b_1^2b^4I_0\omega^8n_2dR_mk}. \tag{43}$$

By graphical analysis similar to Fig. 2, we can find a set of parameters which yield optical bistability. Numerical determinations of solutions A_0 and A_2 show that optical bistability in such a configuration is strongly dependent on z, z_1, R, f, and especiallly on ω_0. The results are shown in Figs. 5(a) and 5(b). The parameters we used for the calculation are $\omega=0.02$ cm, $\lambda=5145$ Å, $R=1000$ cm, $z=12.5$ cm, $z_1=17$ cm, and $f=10$ cm, which are *identical to the experimental situation in which bistability is observed.*

EXPERIMENT

We have performed a quantitative experiment of intensity distribution bistability using nematic film as a nonlinear medium in conjunction with a cw argon ion laser. The experimental setup is depicted in Fig. 1. The mirror used has a reflectivity $R=99\%$. The size of the pin-hole (0.04 mm) relative to the beam diameter is 1:14 at the detector plane. The size, and radial location of this pinhole (besides other parameters), decides to a large extent the output and/or input curve (e.g., powers at switch-up and down, size of the hysteresis, multiple switchings, etc.). The liquid-crystal film used is a homeotropically aligned (room temperature) PCB (pentylcyano-biphenly) film about 50 μm thick oriented such that the director axis makes an angle of 22.5° (an air to glass-slides angle of 45°) with the optical propagation direction. The Ar^+ laser used is linearly polarized. For this geometry, $\bar{n}_2$ [as defined in (2)] is estimated to be 3×10^{-5} $(W/cm^2)^{-1}$. The power of the incident laser is varied from 0 to 1 W, a complete scan takes about 10 min. (i.e., a very slow one). This is because for the 50-μm liquid crystal used, the reorientation response time is on the order of 2 sec. As a result of this slow response time, one can *visually* see the dynamics of the switching process by observing the laser intensity just before the pinhole. In general, when switching occurs, the central portion of the beam is highly intensified, and one or two rings begin to appear (cf. Fig. 1 photo before the pinhole).

Figure 6 shows a typical output versus input curve when the pinhole is located on-axis, with a relative size (pinhole diameter:beam waist) of 1:14. This pinhole size collects all the light at the visibly intensified central area. Switch-up was observed at an input power of 1 W. The spot size of the *incident* laser was estimated to be 0.3 mm, which is also roughly the size of the reflected (feedback) beam. This corresponds to a switch-up intensity of 500 W/cm^2. The switch-up time is observed to be about 3 sec. Switch-down occurred at an incident power of 0.6 W (intensity of 300 W/cm^2). This switching behavior agrees remarkably with the theoretically predicted behavior for the same set of parameters used ($z=12.5$ cm, $z_1=12.5$ cm). More importantly, the calculated (based on the acutal ex-

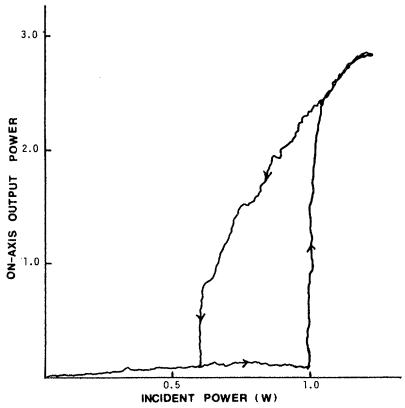

FIG. 6. Experimentally measured output vs input power showing bistability switching.

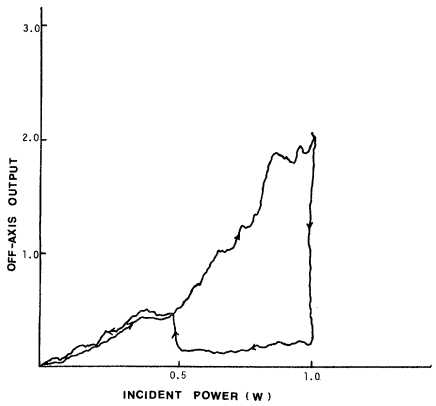

FIG. 7. Experimentally measured output vs input power for the pinhole located at where the dark ring (in the Fig. 1 photo) will occur, showing reverse switchings.

perimental parameters) switching powers agree to within a factor of 6 of the experimental values (theoretical switch-up intensity is lower and is 80 W/cm^2). The slightly higher experimental values for the switching power can be attributed to several factors. For example, because the liquid-crystal film is sandwiched between two microscope slides, there are at least 8% of the incident as well as the reflected (feedback) laser that is lost. The liquid-crystal film itself introduced some further scattering loss. Nevertheless, the overall shape and size of the hysteresis curve agrees well with the theoretical results.

When switch-up occurs at the on-axis region, dark rings appear at the rim of the central bright spot (cf. Fig. 1). Visually, one can see a gradual decrease in the optical intensity in this region, while the center spot intensifies, i.e., a transfer or redistribution of the optical energy at the detector plane. This behavior can also be theoretically deduced from Eqs. (37) and (38). To investigate this, we move the pinhole to where the dark ring occurs and monitor the intensity here as a function of the incident laser power. Figure 7 depicts a typical observed trace. The switch-down occurs at exactly the power for switch-up at the on-axis, and vice versa.

The success of the transverse bistability switching depends critically on the alignment. If the feedback is not exactly back on the spot illuminated by the incident laser, then the transmitted intensity distribution is no longer radially symmetric. Occasionally, one can see two bright near axis spots which collapse into a single one or break up into several spots at higher laser power. For this configuration, the output and/or input curve exhibits very complicated hysteresis effects with (or without) multiple "switching" behavior.

The intensity distribution is extremely dependent on the parameter z for a fixed focal length of the lens, and also on z_1. Bistability switchings occur only for a range of values of z near $z=12$ cm. In general, if the feedback beam spot size is much larger than the incident beam, we do not observe any switching.

CONCLUSION

We have presented a theory of transverse intensity distribution bistability in the transmission of a cw Gaussian laser beam through a nonlinear thin film. Experimental results are obtained for the case where the nonlinear film is a homeotropically aligned nematic liquid crystal and the nonlinearity is the optically induced refractive index change associated with director axis reorientation. Good agreement is obtained between theoretical predictions and experiment. The theory is generally applicable for thin films with an intensity dependent refractive index. The experiments demonstrate that such "weak" or "external" self-focusing optical intensity distribution bistability can be quantitatively described and thus the phenomenon will be an interesting candidate for device application, if faster response media are used. It is important to note here, nevertheless, that further extensive calculations of the switching curves have shown that they are, in general, very sensitive to the parameters ω, z, z_1. For example, if ω changes by a few percent, the switching curves (powers, etc.) change considerably. There are, however, clearly defined ranges of values for these parameters where the switching curves fall unambiguously into the differential gain mode, the bistable mode, the power limiting mode, etc. A complete theoretical analysis of these effects and their experimental verifications will be published later.

ACKNOWLEDGMENTS

This research was supported by a grant from the National Science Foundation, No. ECS-80-26775.

APPENDIX

We consider in this section the effect of including the total phase shift associated with the incident laser, while retaining the first two terms in the feedback, i.e., Eq. (14) now becomes

$$\delta\phi=\bar{n}_2 dI_0 \exp\left[-\frac{r^2}{\omega^2}+\bar{n}_2 dR_m(A_0+A_2 r^2)\right]. \tag{A1}$$

The intensity $I(r_0,z)$ is now given by, after some algebra.

$$I(r_0,z)=\left[\frac{k}{z}\right]^2 I_0\left|\int_0^\infty dr\, rJ_0(krr_0/z)\exp\left\{-ik\left[\frac{r^2}{2z}+\frac{r^2}{2R}+n_2I_0d\exp\left[-\frac{2r^2}{\omega^2}\right]-n_2dR_mA_2\right]\right\}\right|^2 . \tag{A2}$$

This gives

$$I(r_0,z)=\left[\frac{k}{z}\right]^2 I_0\left|\sum_{n=0}^{\infty}\frac{(-1)^nD^n}{2n!(B+Gn)}\exp\left[-\frac{k^2r_0^2/4z^2}{B+Gn}\right]\right|^2 ,$$

where

$$D=ikn_2I_0d,\quad G=2/\omega^2 ,$$
$$B=1/\omega^2+ik(1/2z+1/2R-n_2dR_mA_2) . \tag{A3}$$

The output $I(r_0,z)$ from (A2) gives a near axis intensity of the form

$$A_0=\left[\frac{k}{z}\right]^2 I_0\left|\sum_{n=0}^{\infty}\frac{(-1)^nD^n}{2n!(B+Gn)}\right|^2 , \tag{A4}$$

$$A_2=\left[\frac{k}{z}\right]^4 I_0\left[\sum_{n=0}^{\infty}\frac{(-1)^nD^n}{2n!(B+Gn)}\sum_{m=0}^{\infty}\frac{(-1)^nD^{*n}}{2m!(B^*+Gm)^2}+\sum_{n=0}^{\infty}\frac{(-1)^nD^{*n}}{2n!(B^*+Gn)}\sum_{m=0}^{\infty}\frac{(-1)^mD^m}{2m!(B+Gm)}\right] , \tag{A5}$$

where

$$\sum_{n=0}^{\infty}\frac{(-1)^nD^n}{n!(B+Gn)}=\sum_{n=0}^{\infty}\frac{D'^ne^{-in\pi/2}}{n!\left|\frac{2n+1}{\omega^2}+ik\left[\frac{1}{2z}+\frac{1}{2R}-n_2dR_mA_2\right]\right|}$$
$$=\sum_{n=0}^{\infty}\frac{D'^ne^{-\pi i/2}e^{i\phi_n}}{n!\left[\left[\frac{2n+1}{\omega^2}\right]^2+k^2\left[\frac{1}{2Z}+\frac{1}{2R}-n_2dR_mA_2\right]\right]^{1/2}} ,$$

$$\phi_n=-\tan^{-1}\frac{k\omega^2\left[\frac{1}{2z}+\frac{1}{2R}-n_2dR_mA_2\right]}{2n+1} ,$$

$$D'=n_2I_0dk .$$

Similarly,

$$\sum_{m=0}^{\infty}\frac{(-1)^mD^{*m}}{m!(B^*+Gm)^2}=\sum_{m=0}^{\infty}\frac{D'^me^{i(\pi/2)m}e^{-i2\phi_m}}{m!\left|\left[\frac{2n+1}{\omega^2}\right]^2+k^2\left[\frac{1}{2z}+\frac{1}{2R}-n_2dR_mA_2\right]^2\right|} ,$$

where if we now define a variable of

$$u=k\omega^2(1/2z+1/2R-n_2dR_mA_2) , \tag{A6}$$

we again obtain a transcendental equation after some lengthy algebra:

$$\beta_1-\beta_2u=(Y_1Y_3+Y_2Y_4)D' , \tag{A7}$$

where

$$Y_1=\sum_{n=0}^{\infty}\frac{D'^n\cos(\phi_n-\pi n/2)}{n![(2n+1)^2+u^2]^{1/2}} ,$$

$$Y_2=\sum_{n=0}^{\infty}\frac{D'^n\sin(\phi_n-\pi n/2)}{n![(2n+1)^2+u^2]^{1/2}} ,$$

$$Y^3=\sum_{n=0}^{\infty}\frac{D'^n\cos(2\phi_n-\pi n/2)}{n![(2n+1)^2+u^2]} ,$$

$$Y_4=\sum_{n=0}^{\infty}\frac{D'^n\sin(2\phi_n=\pi n/2)}{n![(2n+1)^2+u^2]} ,$$

$$\phi_n=-\tan^{-1}\left[\frac{u}{(2n+1)}\right] , \tag{A8}$$

$$D'=\bar{n}_2I_0dk ,$$

$$\beta_1=\left[\frac{4z^4}{k^3\omega^6R_m}\right](1/z+1/k) ,$$

$$\beta_2=\frac{8z^4}{k^4\omega^8R_m} .$$

The lhs of Eq. (A7) depends on u and the physical parameters like R, z, R, ω (but not on z_0) while the rhs depends on u and I_0 (in particular). We have, again, a transcen-

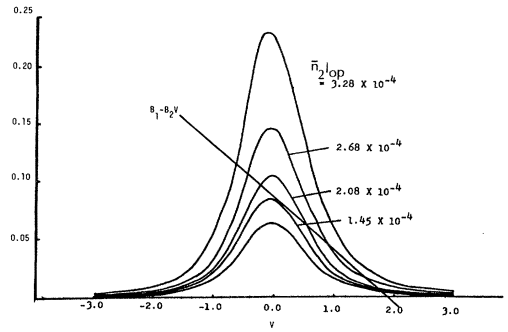

FIG. 8. Theoretical plot of $y=(Y_1Y_3+Y_2Y_4)D'$ and $y=B_1-B_2V$ for various values of $\bar{n}_2 I_{op}$, when the total phase shift due to the input beam is taken into account.

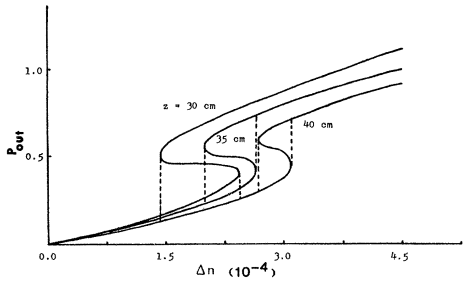

FIG. 9. Corresponding output vs input power bistability switching showing much resemblance to Fig. 3 where only the near-axis phase shift is included in the calculation.

dental equation involving a straight line and a bell-shaped function. Figure 8 is a plot of the Eq. (A7) for values of I_0 corresponding to $\Delta n=3.28\times10^{-4}$, 2.68×10^{-4}, 2.08×10^{-4}, and 1.45×10^{-4} for the same set of parameters used in Fig. 2. Notice that as a result of the different defintion for u here [Eq. (A6)] and u in the text [Eq. (19)], the slope and the intercept of the straight line does not change with I_0, while it is the bell-shaped function that varies both in amplitude and in width with I_0. However, when the values obtained from these intersections in Fig. 8 are used to plot the power at the pinhole versus the input (in terms of Δn) as shown in Fig. 9, we notice that there is very little difference in the bistability switching curves for the same set of parameters compared to Fig. 3 obtained in the text. One conclusion that one may make, therefore, is that the major contribution to the first bistability switching loop is from the near axis optical intensity.

*Present address: Physics Department, Pennsylvania State University, University Park, PA 16802.

†Present address: Hua Zhong University of Technology, Wuhan, The People's Republic of China.

[1]J. E. Bjorkholm, P. W. Smith, W. J. Tomlinson, and A. E. Kaplan, Opt. Lett. 6, 345 (1981); J. E. Bjorkholm, P. W. Smith, and W. J. Tomlinson, IEEE J. Quantum Electron. QE-18, 2016 (1982).

[2]A. E. Kaplan, Opt. Lett. 6, 360 (1981).

[3]For a comprehensive review, see *Optical Bistability,* edited by C. M. Bowden, M. Cifton, and H. R. Robl (Plenum, New York, 1980) and references therein.

[4]H. M. Gibbs, S. L. McCall, and T. N. C. Venktesan, Phys. Rev. Lett. 36, 1135 (1976); see also Ref. 3 for various other works by Gibbs and co-workers.

[5]F. S. Felber and J. H. Marburger, Appl. Phys. Lett. 28, 731 (1976); Phys. Rev. A 17, 335 (1978).

[6]I. C. Khoo, J. Y. Hou, R. Normandin, and V. C. Y. So, Phys. Rev. A 27, 3251 (1983).

[7]T. Bischoffberger and Y. R. Shen, Appl. Phys. Lett. 32, 156 (1976); Phys. Rev. A 19, 1169 (1979).

[8]A preliminary experimental observation has been reported by I. C. Khoo, Appl. Phys. Lett. 41, 909 (1982).

[9]I. C. Khoo, Phys. Rev. A 25, 1636 (1982); 27, 2747 (1983).

[10]See, for example, J. W. Goodman, *Introduction to Fourier Optics* (McGraw-Hill, New York, 1968).

[11]P. Y. Yan, thesis, Wayne State University, 1983.